

Finite element modelling of tensile reinforcement laps in steel fibre reinforced concrete

P. Grassl & J. Middlemiss

School of Engineering, University of Glasgow, Glasgow, UK

ABSTRACT: For being able to design tensile reinforcement laps with confidence, a good understanding of the mechanical performance and failure process is required. In this study, the response of laps subjected to tension in plain and steel fibre reinforced concrete was investigated by nonlinear finite element analyses. For analysing reinforced concrete, the individual phases of the composite, namely concrete, steel and bond between steel and concrete, were modelled. For concrete, a damage-plasticity constitutive model was used. The stress-crack opening curve of concrete was calibrated to describe the influence of steel fibres on the cracking response. The results show that a small volume fraction of fibres improves the mechanical performance of tensile reinforcement laps significantly.

1 INTRODUCTION

In reinforced concrete structures, connections between members are often critical for the performance of structural systems in the ultimate limit state. A common approach for providing force transfer across two structural concrete members is to overlap reinforcement bars. However, equations in design codes for determining the required lap length for these connection differ significantly (Micallef and Vollum 2018, Cairns 2015, Vollum and Goodchild 2019). A possible explanation for this discrepancy is that the the strongly nonlinear response of these reinforcement laps involves complex failure processes, which might not be fully understood yet.

The nonlinear finite element method provides a powerful tool for investigating the nonlinear response of reinforced concrete structures (de Borst et al. 2012). By modelling separately the nonlinear response of concrete, steel and bond between concrete and steel, it is possible to provide a better understanding of the processes which govern the often highly nonlinear composite response. However, for being able to interpret the results of nonlinear finite element analyses with confidence, it is required to provide constitutive models for the different phases of reinforced concrete, which reproduce experimental results well. Furthermore, the employed numerical solution strategy of the nonlinear finite element method has to be robust. By far the most challenging phase to model is concrete with its quasi-brittle response in tension and low-confined compression, and ductile response in highly confined compression.

The aim of the present study is to investigate the influence of concrete properties on reinforcement laps subjected to direct tension by nonlinear finite element analyses. The analyses were performed with an explicit solution strategy and a damage-plasticity constitutive approach CDPM2 for concrete proposed in Grassl et al. (2013). In the damage-plasticity model, the input for the tensile response of concrete is given in the form of a stress-versus crack-opening curve. It was adjusted to model two types of material in the form of plain concrete and concrete with steel fibres.

2 METHOD

The nonlinear analysis of reinforcement laps in concrete subjected to tension were performed by means of an explicit dynamic solution approach using incremental displacement control. Concrete, reinforcement and interaction between concrete and reinforcement were modelled separately. For concrete, constant stress tetrahedral finite elements were used. Reinforcement was modelled by frame elements which were positioned independently of the finite element mesh of concrete. The interaction between concrete and reinforcement was modelled by linking the degrees of freedom of frame elements to those of the concrete elements (Phillips and Zienkiewicz 1976), while enforcing bond-slip laws between reinforcement and concrete. Nonlinear constitutive models for concrete, steel and interaction between concrete and steel were used, which are described in the following paragraphs.

For concrete, the damage-plasticity model

CDPM2, which was proposed by the first author in Grassl et al. (2013), was used. This model is based on a previously developed damage-plasticity approach in Grassl and Jirásek (2006). In CDPM2, the stress evaluation is based on the damage mechanics concept of nominal and effective stress. The nominal stress is evaluated by a combination of damage and plasticity, whereas the effective stress in the undamaged material is determined using plasticity. For the nominal stress evaluation, tensile and compressive damage variables are applied to positive and negative components of the principal effective stress, respectively.

The plasticity part of the model is formulated in the effective stress space. The yield surface is based on the strength envelope proposed in Menétrey and Willam (1995), which provides a good agreement with experimental results for multiaxial tensile and compression tests of plain concrete. In the principal stress space, this strength envelope is characterised by curved meridians and deviatoric sections varying from almost triangular in tension to almost circular in highly confined compression. Damage is initiated once the strength envelope is reached. Then, the response is a combination of plasticity and damage. Evolution laws for tensile and compressive damage variables are formulated as functions of positive and negative parts of the principal effective stress so that tensile and compressive softening responses can be described independently of each other. The function for the tensile damage variable is derived from a bilinear stress-crack opening (σ - w_c) curve, so that the results of analyses of tensile failure in which strains localise in mesh-dependent regions are independent of the finite element mesh (Pietruszczak and Mróz 1981, Bažant and Oh 1983, Willam et al. 1986). The compressive damage variable is linked to a stress-inelastic strain curve, since the deformation patterns in the compressive zones of bending dominated applications are often mesh-size independent (Grassl et al. 2013).

The damage-plasticity model requires many input parameters, which can be divided into groups related to the elastic, plastic and damage parts of the model. In the present work, most of these parameters are set to their default values provided in (Grassl et al. 2013), where it was shown that they provide a good match with experimental results. Some of the parameters which are directly linked to experimental results, such as Young's modulus E , Poisson's ratio ν , compressive strength f_c , and parameters of the bilinear stress-crack opening curves, f_t , f_{t1} , w_{f1} and w_f , were adjusted to match the response of concrete and concrete with fibres. Here f_t and f_{t1} are the tensile strength at peak and the stress at the change of slope, respectively. The parameters w_{f1} and w_f are the crack openings at the change of slope and at the stage when zero stress is reached, respectively. For concrete without fibres, the four parameters were chosen so that the area under

the stress-crack opening curve matches the fracture energy G_F of concrete with default values of ratios f_{t1}/f_t and w_{f1}/w_f proposed in Grassl et al. (2013). For fibre reinforced concrete, the parameters f_t , f_{t1} and w_f were adjusted to consider the bridging effects of the fibres using rules proposed in Naaman (1987, Naaman et al. (1991). Here, it was assumed that the steel fibres, which bridge a crack, are pulled out of the concrete, but do not yield. The presence of small steel fibre volume ratios considered in this study resulted in a small increase of f_t and f_{t1} , and a very large increase of w_f . The parameter w_{f1} was kept for fibre reinforced concrete the same as for concrete without fibres.

For the reinforcement and bond concrete and reinforcement, simpler constitutive models were used. The constitutive model for the reinforcement was chosen to be elasto-plastic without hardening. The required parameters are the Young's modulus E , Poisson's ratio ν and yield strength σ_y . For the interaction between concrete and reinforcement, a nonlinear bond-slip law was chosen, so that the bond stress remains constant once it has reached the maximum value τ_{max} . The initial slope of the hardening response was set to a high value.

3 ANALYSIS AND RESULTS

Connections made of straight reinforcement bars in concrete subjected to direct tension were analysed using the modelling approach described in the previous section. The specimen, shown in Figure 1, consists of concrete with four symmetrically arranged reinforcement bars lapped at the centre of the specimen.

The influence of lap length L_s and material properties (concrete with and without fibres) were studied. Loading was applied by prescribing axial displacement at one end of the reinforcement bars, while supporting the other end. The displacement rate was set to a small enough value so that dynamic effects were not important. The diameter of the middle part of the reinforcement bars was $\phi = 20$ mm. The ends of the four reinforcement bars were made of twice this diameter so that yielding of the reinforcement at the end of the specimen was avoided (Figure 1). This was particularly important for specimens made of fibre reinforced concrete, for which fibres contribute significantly to the load transfer across tensile cracks. The material input for concrete without fibres was chosen as $E = 35$ GPa, $\nu = 0.2$, $f_c = 40$ MPa, $f_t = 3$ MPa, $f_{t1} = 1.27$ MPa, $w_{f1} = 0.0177$ mm and $w_f = 0.118$ mm. These parameters are typical for plain concrete (CEB-FIP12 2012). The input for the stress-crack opening curve results in a fracture energy of $G_F = 142$ J/m². For concrete with a steel fibre volume fraction of $V_f = 0.01$, the material parameters were $E = 35$ GPa, $\nu = 0.2$, $f_c = 40$ MPa, $f_t = 3.22$ MPa, $f_{t1} = 1.27$ MPa, $w_{f1} = 0.018$ mm and $w_f = 17.5$ mm. These parameters were determined from the plain concrete values and the rules proposed in Naaman (1987, Naaman et al.

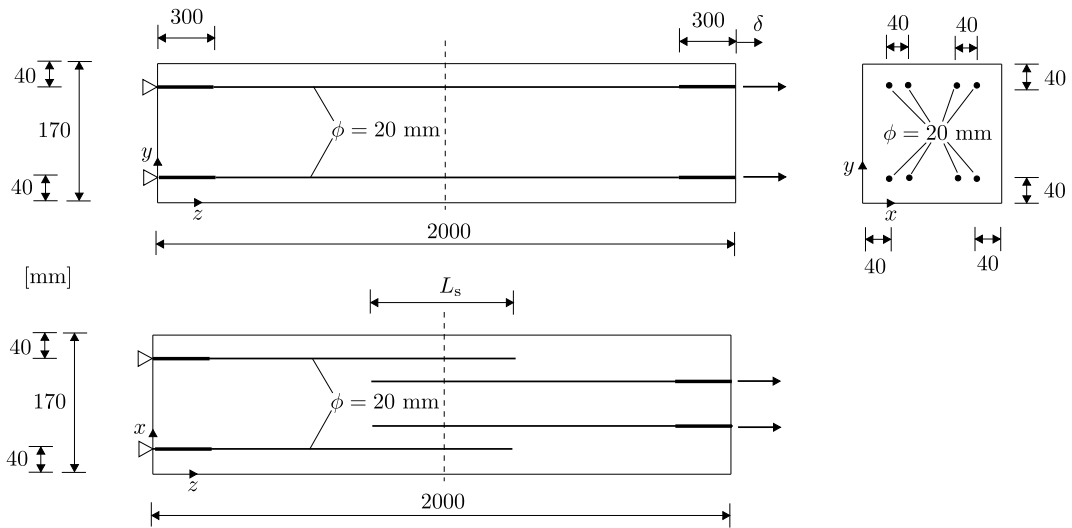


Figure 1: Geometry of the lab splicing in direct tension. The specified dimensions refer to the centre lines of the reinforcement bars.

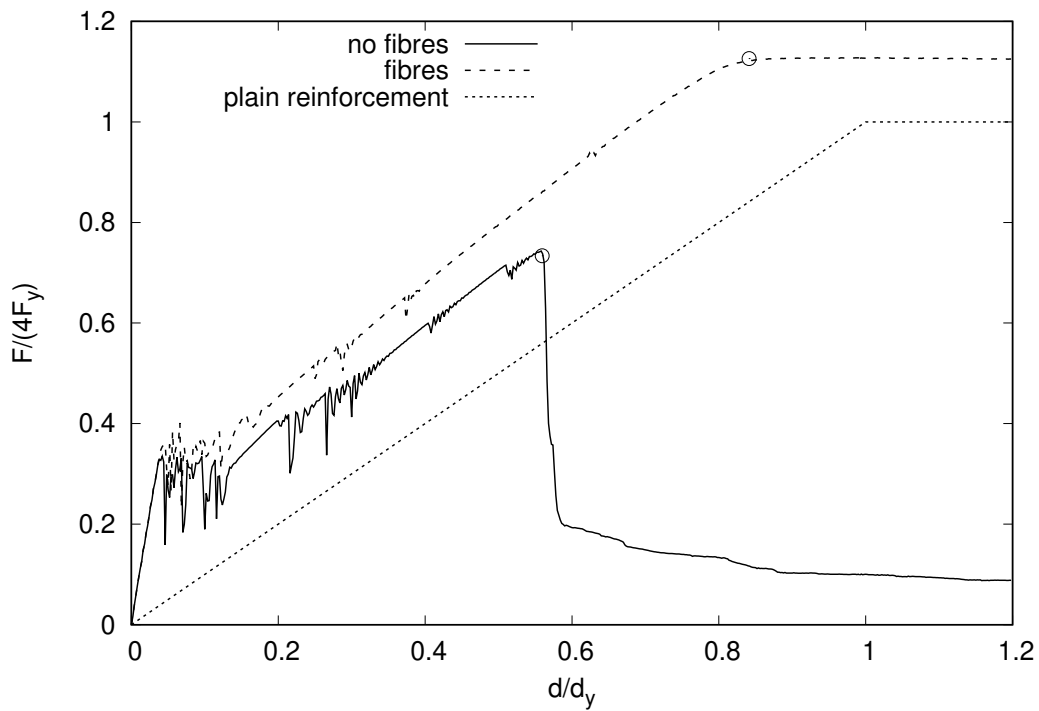


Figure 2: Load-displacement curves for straight reinforcement laps in concrete with a lap length of $L_s = 500 \text{ mm}$ with and without fibres obtained from nonlinear finite element analyses with the concrete damage plasticity model CDPM2.

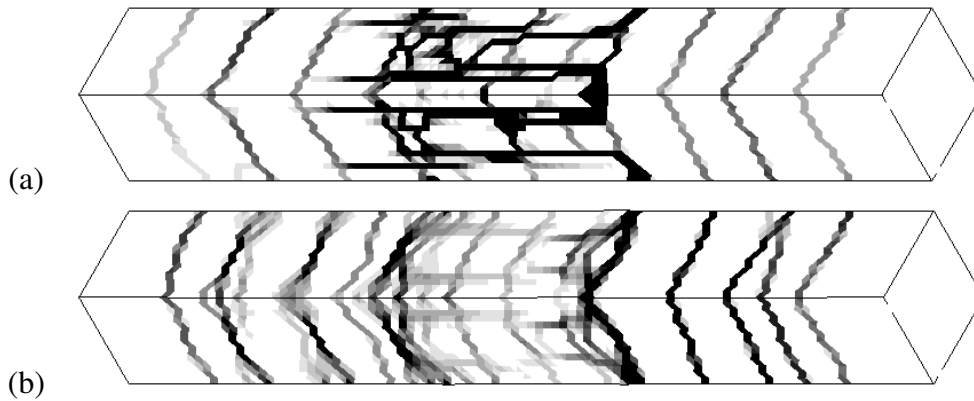


Figure 3: Contour plots of the maximum principal strain for lab splices (a) without fibres and (b) with fibres. Black indicates strains which correspond to crack openings greater than 0.3 mm.

(1991). For the reinforcement, the yield strength was set to $\sigma_y = 500$ MPa. The maximum bond stress was $\tau_{\max} = 15.81$ MPa.

In this short paper only selected results for one short lap length $L_s = 500$ mm with and without fibres are shown in the form load-displacement curves (Figure 2) and contour plots of principle strains (Figure 3). For the load-displacement curves in Figure 2, the load and displacement are normalised by the force and displacement of four plain reinforcement bars at yielding, respectively. The first main cracks occur at approximately 30% of the yield force of the reinforcement. After cracking, the slope of the load-displacement curve is reduced. Still, the displacement is still less than for the plain reinforcement bars at the same load, because concrete contributes to the load transfer between cracks. For concrete without fibres, the peak load is reached before the reinforcement bars yield, which indicates that the strength of the lap limits the overall strength of the specimen. The post-peak response is characterised by a sudden drop of the load. For concrete with fibres, the peak load exceeds the yield load of the reinforcement. In the post-peak regime, the load remains constant. This response indicates that yielding of the reinforcement limits the strength of the specimen. The maximum load is greater than the yield load of the steel, since the bridging stress of steel fibres across cracks contribute to the load transfer.

The crack patterns in Figure 3a and b are shown at maximum load (marked in Figure 2) for concrete without and with fibres, respectively. Overall, the crack patterns for the two cases are very similar. Outside the lap zone, tensile cracks perpendicular to the load direction are visible. Within the lap zone, both perpendicular and longitudinal cracks are present. The occurrence of longitudinal splitting cracks is in agreement with crack patterns observed in experiments (Micallef and Vollum 2018). There are differences in the magnitude of crack openings for the two materials. For the case without fibres, cracks with large openings are concentrated in the lap zone.

Despite the qualitatively very similar crack patterns in Figure 3, the load displacement curves in Figure 2 for the two cases are very different. It should be remembered that the volume fraction of steel fibres ($V_f = 1\%$) is so low, that the peak stress in tension is not significantly increased ($f_t = 3.22$ MPa for fibre reinforced concrete versus $f_t = 3$ MPa for plain concrete). Therefore, the initial crack patterns do not differ significantly. However, for fibre reinforced concrete, the bridging stress after cracking is maintained for a very large range of crack opening. This bridging stress is sufficient to provide enough tensile resistance for the lap to transfer load, which is large enough to cause yielding of the reinforcement.

4 CONCLUSIONS

The present nonlinear finite element analyses of a short tensile reinforcement lap in both plain and steel fibre reinforced concrete show that 1 % of volume fraction of steel fibres has a strong influence on the mechanical response of the tensile lap. For plain concrete, splitting cracks result in an abrupt drop of the load before yielding of the reinforcement occurs. On the other hand, for steel fibre reinforced concrete, the formation of splitting cracks does not result in this drop. Instead, the load increases further until yielding of the reinforcement occurs.

REFERENCES

- Bažant, Z. P. & B.-H. Oh (1983). Crack band theory for fracture of concrete. *Materials and Structures* 16, 155–177.
- Cairns, J. (2015). Bond and anchorage of embedded steel reinforcement in fib model code 2010. *Structural Concrete* 16(1), 45–55.
- CEB-FIP12 (2012). *CEB-FIP Model Code 2010, Design Code*.
- de Borst, R., M. Crisfield, J. J. C. Remmers, & C. V. Verhoosel (2012). *Nonlinear finite element analysis of solids and structures*. John Wiley & Sons.
- Grassl, P. & M. Jirásek (2006). Damage-plastic model for concrete failure. *International Journal of Solids and Structures* 43, 7166–7196.
- Grassl, P., D. Xenos, U. Nyström, R. Rempling, & K. Gylltoft (2013). CDPM2: A damage-plasticity approach to modelling the failure of concrete. *International Journal of Solids and Structures* 50(24), 3805–3816.
- Menétrey, P. & K. J. Willam (1995). A triaxial failure criterion for concrete and its generalization. *ACI Structural Journal* 92, 311–318.
- Micallef, M. & R. L. Vollum (2018). The behaviour of long tension reinforcement laps. *Magazine of Concrete Research* 211(1), 739–755.
- Naaman, A. E. (1987). High performance fibre reinforced cement composites. *IABSE reports* 55, 371–376.
- Naaman, A. E., G. G. Namur, J. M. Alwan, & H. S. Najm (1991). Fiber pullout and bond slip. I: Analytical study. *Journal of Structural Engineering* 117(9), 2769–2790.
- Phillips, D. V. & O. C. Zienkiewicz (1976). Finite element nonlinear analysis of concrete structures. In *Institution of Civil Engineers, Proceedings*, Volume 61.
- Pietruszczak, S. T. & Z. Mróz (1981). Finite element analysis of deformation of strain-softening materials. *International Journal for Numerical Methods in Engineering* 17(3), 327–334.
- Vollum, R. & C. Goodchild (2019). Proposed en 1992 tension lap strength equation for good bond. *Structures* 19, 5–18.
- Willam, K., N. Bićanić, & S. Sture (1986). Composite fracture model for strain-softening and localised failure of concrete. In E. Hinton and D. R. J. Owen (Eds.), *Computational Modelling of Reinforced Concrete Structures*, Swansea, pp. 122–153. Pineridge Press.